Comparative Flexural Behavior of Precast Beam Joint Loop and Loop-Pin Models under Static Loads

Israel Padang
Civil Engineering Department, Hasanuddin University, Indonesia
civilrael1107@gmail.com (corresponding author)

Rudy Djamaluddin
Civil Engineering Department, Hasanuddin University, Indonesia
rudy0011@gmail.com

Herman Parung
Civil Engineering Department, Hasanuddin University, Indonesia
parungherman@yahoo.co.id

Received: 16 October 2025 | Revised: 10 November 2025 | Accepted: 21 November 2025

 DOI: https://doi.org/10.48084/etasr.15591

ABSTRACT

This study investigates the flexural behavior of Precast Beams with two connection models—Loop (PB-L) and Loop-Pin (PB-LP)—compared to a Monolithic Beam (MB) as the control. Experimental flexural tests were conducted using a two-point static loading setup. The key parameters analyzed include initial flexural capacity (Pcr, Mcr), yield capacity (Py, My), ultimate capacity (Pu, Mult), deflection (Δcr, Δy, Δult), as well as steel and concrete strain behavior. The PB-LP beam exhibited the highest initial stiffness and cracking load capacity (Pcr = 9.42 kN; Mcr = 6.66 kNm), approximately 65% higher than MB, but showed lower steel and concrete yield strain compared to PB-L and MB. Conversely, PB-L closely matched the MB in terms of yield and ultimate capacities. All beam specimens achieved ductility ratios between 7 and 7.4, which classified them as high-ductility elements, indicating adequate plastic deformation capacity for seismic applications. These findings demonstrate that both loop and loop-pin connections are viable for precast systems in low-cost housing in seismic regions, with PB-L providing monolithic-like behavior and PB-LP excelling in initial crack resistance.

Keywords-precast beam; loop connection; loop-pin connection; flexural capacity; ductility

I. INTRODUCTION

Indonesia, located within the Pacific Ring of Fire, a subduction zone between the Indo-Australian, Eurasian, and Pacific plates, has a high level of vulnerability to earthquakes and volcanic eruptions [1]. Data from the National Disaster Management Agency (BNPB) indicate that between January 2020 and October 2025, thousands of disasters occurred across the country, resulting in 3138 fatalities and affecting or displacing more than 42 million people. The housing sector was among the most severely impacted, with 478737 housing units damaged, including 312125 lightly damaged, 89261 moderately damaged, and 77351 severely damaged houses [2]. These conditions highlight the urgent need for rapid, efficient, and high-quality post-disaster housing reconstruction. In this context, the precast concrete system offers a promising solution, as it enables faster construction and ensures quality through factory-controlled production. However, despite its potential, the current implementation of precast systems in low-cost housing reconstruction remains limited. This is due to inadequate connection technology and high dependence on conventional cast-in-place detailing, which reduces efficiency and increases cost. Precast components can also be designed to support earthquake-resistant structures through lightweight, symmetrical configurations and rational reinforcement continuity [3, 4]. Despite the advantages of precast systems, their primary challenge lies in designing effective connections between structural elements. These connections must safely transfer both gravity and lateral loads while preserving overall structural integrity [5]. Conventional approaches typically use mechanical joints and reinforcement details that mimic cast-in-place concrete behavior [4, 6]. However, in the context of low-cost, post-disaster housing reconstruction, such detailing can become costly and complicated, ultimately slowing down construction efforts [7].

Research has explored innovative joint technologies to overcome these limitations. For example, an in-span UHPC joint was developed to mitigate stress concentrations and enhance beam performance [8], while unbonded post-tensioned PB using recycled aggregate concrete demonstrated improved material efficiency [9]. Authors in [10] highlighted mechanical and self-centering connections as promising strategies to reduce reinforcement congestion in joint regions. At the member level, hybrid UHPC–NSC beams exhibited improved initial stiffness [11]. Conversely, UHPC segmental beams incorporating epoxy joints and unbonded tendons exhibited 9%–15% lower flexural strength than their monolithic counterparts, indicating the critical role of joint design and quality [12]. Several parameter studies have further investigated how joint geometry and reinforcement detailing influence flexural behavior. Joint length has been found to significantly affect flexural capacity [13], while dowel-type beam–column connections demonstrated stable hysteretic responses under cyclic lateral loading [14]. Increasing reinforcement ratios in precast lightweight elements correlates positively with flexural strength [15]. Additionally, the use of recycled glass as a sand substitute in reinforced concrete beams enriches discussions on material efficiency and flexural behavior enhancement [16]. However, wet-joint polymer-concrete beams generally exhibit lower flexural capacity than MBs, underscoring the sensitivity of structural performance to joint geometry and construction quality [17]. As part of innovations in precast connection technology, this study focuses on developing a connection system using vertical loop reinforcement (tension–compression reinforcement). This system is expected to be more effective in enhancing flexural capacity compared to conventional joints. Authors in [18] reported that steel loop bars used to connect two precast concrete elements, subsequently filled with grouting as a bonding material, were effective in ensuring structural integrity, reducing on-site work, minimizing construction costs, and improving flexural performance. However, the overall behavior was strongly influenced by joint geometry. Moreover, the loop system can replace on-site welding by providing strong mechanical interlocking, accelerating installation, and increasing assembly tolerance [19]. Increasing the overlap length has also been shown to improve flexural strength and produce ductile failure with fewer cracks [20].

For further development of the loop system, this study explores the integration of a horizontal pin within the curvature of the loop reinforcement to enhance the flexural performance of precast beam joints and to address the weaknesses observed in previous studies, where cracking occurred in the joint region. This concept aligns with [21], where it was demonstrated that incorporating mechanical interlocking components in wet joints can enhance force transfer efficiency, mitigate slip between connected elements, and improve the overall ductility of precast concrete connections. Authors in [22] examined horizontal loop connections considering parameters, such as overlap length, internal loop diameter, interface roughness, and the percentage of cottering bars (i.e., dowel-like bars providing mechanical interlock), and reported increases in flexural capacity along with an empirical expression for the moment capacity. Although the performance of loop connections in precast elements has been extensively investigated, a major issue is the occurrence of cracking in the joint region due to high stress concentrations. This problem limits the wider application of loop-type joints in affordable seismic-resistant housing, where both structural reliability and construction efficiency are critical requirements. Based on this limitation, the present study proposes the development of a loop connection by adding a horizontal pin within the loop curvature as an additional mechanical interlock to enhance the effectiveness of force transfer between elements. Adding reinforcing pins to loop connections can improve the flexural capacity, ductility, and crack control of precast beam joints. The pins enhance mechanical interlock and help reduce stress concentrations within the joint region. This improvement makes the system a practical and efficient option for constructing low-cost, earthquake-resistant housing.

II. EXPERIMENTAL WORK

A. Specimen Design and Fabrication

This experimental study was conducted at the Laboratory of Materials and Structures, Department of Civil Engineering, Hasanuddin University. Three types of beam specimens were prepared: MB (control specimen), PB-L precast beam with loop reinforcement connection, and PB-LP precast beam with loop + pin reinforcement connection, as shown in Figures 1-3. These two connection types (loop and loop-pin) were selected due to their practicality, ease of assembly, and compatibility with modular precast components in low-cost housing applications. Each beam specimen had dimensions of 150 mm × 250 mm × 3300 mm, with a joint located at mid-span for PB-L and PB-LP. The joint length was set to h = 250 mm and grouted using Sika Grout 215 to ensure proper bonding between elements. The reinforcement details (tension and compression bars, stirrups, and loop/pin configuration) were designed in accordance with [23] and are summarized in Table I. The selected beam dimensions were determined based on the provisions of [23], where the minimum requirements for flexural members in reinforced concrete design are specified. The reinforcement detailing followed the Technical Guideline for Simple Building Construction published by the Ministry of Public Works and Housing, Directorate General of Human Settlements (2022), which represents common practices for low-cost residential structures in Indonesia.

TABLE I. BEAM REINFORCEMENT DETAILS

Specimen	Reinforcement type	As (mm^2)	As'/As (%)	Stirrups	Joint type
MB	Monolithic	157	100	Φ8-125	None
PB-L	Loop	157	100	Φ8-125	Wet-Joint
PB-LP	Loop + Pin	157	100	Φ8-125	Wet-Joint

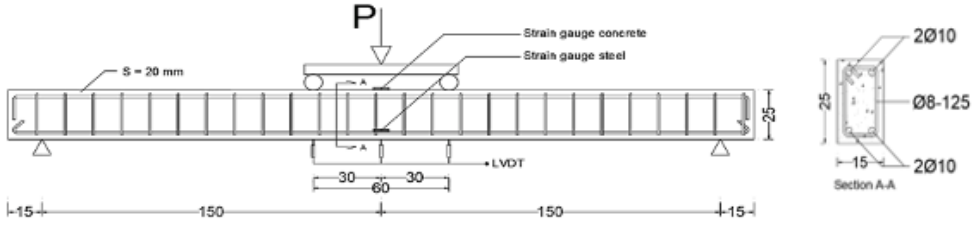

Fig. 1. Design, reinforcement details, loading scheme, and instrumentation layout for the MB. All dimensions are in mm; a scale bar is included.

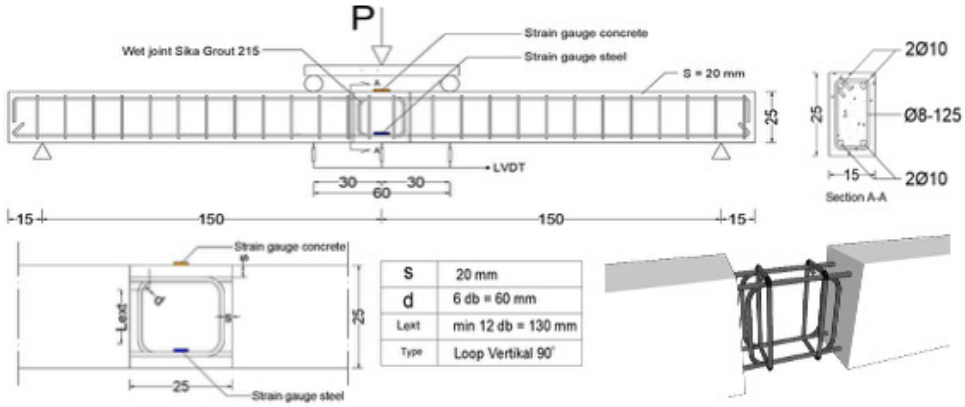

Fig. 2. Design, reinforcement details, loading scheme, and instrumentation layout for the PB-L. All dimensions are in mm; a scale bar is included.

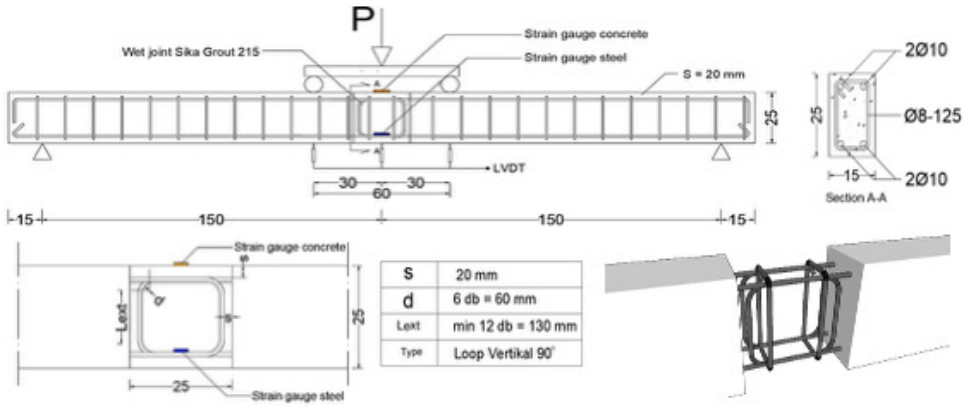

Fig. 3. Design, reinforcement details, loading scheme, and instrumentation layout for the PB-LP. All dimensions are in mm; a scale bar is included.

B. Material Properties

The concrete used in the study was designed for f'c = 25 MPa. The average compressive strength at 28 days was determined by testing three standard cylinders in accordance with the national standard procedure.

TABLE II. MATERIAL PROPERTIES

Material	Property	Test result
Concrete	f'c (MPa)	21.45
Reinforcement	fy (MPa)	431.28
Grout	fc (MPa)	58.94

Reinforcement steel properties (yield and ultimate strength) were obtained from tensile tests. The compressive strength of the grout was tested using mortar cubes, and flowability was measured with a flow table test to ensure proper workability. The results are summarized in Table II. The material tests were conducted before the beam testing to ensure that the materials met the minimum quality requirements. The compressive strength of concrete was determined using standard cylindrical specimens (150 mm × 300 mm) in accordance with [24]. The average test result was 21.45 MPa, which was slightly below the target design strength of 25 MPa but still acceptable for structural concrete, as it exceeds the minimum requirement of 17 MPa for structural-grade concrete, as specified in [23]. The reinforcing steel used was a 10 mm deformed bar, tested for its tensile properties in accordance with [25]. The yield strength (fy) and ultimate strength (fu) were determined from the stress–

strain curve obtained through a direct tensile test, using the 0.2% offset method to define the yield point. The recorded average yield strength was 431.28 MPa. The grout compressive strength was evaluated using 50 mm × 50 mm × 50 mm cube specimens, tested in accordance with [26].

C. Specimen Fabrication

Beam specimens were cast in two stages for precast elements: (1) precast half-beams were cast and cured for 28 days; (2) the joint region was assembled and grouted to form the final beam. For MB, a single monolithic pour was performed. All specimens were cured under moist conditions for 28 days to ensure consistent concrete quality.

D. Loading and Measurement Setup

Flexural testing was performed using a 1500 kN Universal Testing Machine (UTM) under a two-point static loading setup, as shown in Figure 4. The loading span and support configuration followed standardized testing procedures [27]. The test was conducted in load-controlled mode at a rate of 0.02 kN/mm to promote stable crack development and gradual failure under quasi-static conditions. Load, deflection, and strain data were recorded at 1 Hz to ensure consistent and reliable measurements throughout the test. LVDTs were positioned at mid-span and beneath the loading points to measure vertical deflection, while electrical resistance strain gauges were attached to the reinforcement and concrete surface to capture strain responses. The loading configuration for all three beam types is displayed in Figures 1-3.

Fig. 4. A UTM is used for a two-point static loading test.

E. Instrument Calibration

Before testing, all measurement devices were calibrated to ensure accurate data collection. The LVDTs (model CDP-100A, TML, Japan) with a 100 mm measurement range were calibrated using a standard micrometer with ±0.01 mm accuracy. The calibration confirmed a linear correlation between the actual displacement and LVDT output, with a maximum deviation of ±1%. Zero checks were performed before and after testing to ensure reading stability. Strain gauges for reinforcement and concrete, FLKB-2-11-5LJC-F and PL-60-11-5LJC-F (TML, Japan) had gauge factors of 2.09–2.1 ± 1%. Their calibration involved applying incremental loads to standard specimens to verify linearity and sensitivity, followed by zero checks before and after each test to avoid signal drift. The loading stages were consistently defined for all specimens: the cracking load (Pcr) corresponded to the first visible crack in the tensile zone; the yield load (Py) was determined from the inflection point of the load–deflection curve, indicating the onset of steel yielding ($\varepsilon y \approx 2000\ \mu\varepsilon$); and the ultimate load (Pu) was defined as the maximum load sustained before a drop in load-carrying capacity.

F. Data Collection and Analysis

The following procedure was adopted for data analysis:

- Load-Deflection Curves: P–Δ curves for each specimen were plotted.
- Flexural Capacity: First-crack load (Pcr), yield load (Py), and ultimate load (Pu) were determined from the curves.
- Stress–Strain Relationships: Tensile and compressive strain data were used to generate the stress–strain responses of both the steel reinforcement and the concrete. The recorded strains were converted to stresses using the appropriate constitutive models for each material, allowing assessment of actual stress development and comparison of the behavior across the different beam types.
- Ductility: The ductility index Δult/Δy was computed. Δult denotes the lateral/vertical displacement increment measured at the loading point (or at midspan) between stages X and Y, while Δy denotes the yield displacement (displacement at first yield of reinforcement/section).

III. RESULTS AND DISCUSSION

A. Flexural Capacity of Beams

The comparison between the PB-L and PB-LP joint models and the MB in terms of load and moment capacity is presented in Table III.

TABLE III. LOAD AND MOMENT CAPACITY

Type	Load (kN)			Moment (kN.m)		
	Pcr	Py	Pult	Mcr	My	Mult
MB	5.02	18.21	23.74	4.02	11.94	15.26
PB-L	5.29	18.28	24.41	4.18	11.98	15.66
PB-LP	9.42	17.28	23.48	6.66	11.38	15.1

1) Load Capacity

The test results reveal that the MB, used as the control specimen, had a critical load capacity (Pcr) of 5.02 kN, while the PB-L exhibited a slightly higher value of 5.29 kN. The PB-LP demonstrated a significantly higher Pcr of 9.42 kN, indicating that the loop-pin joint enhances the initial stiffness and cracking resistance compared to both the monolithic and loop joint beams. For the yield (Py) and ultimate load capacities (Pult), PB-L (18.28 kN and 24.41 kN) showed values comparable to or slightly higher than MB (18.21 kN and 23.74 kN). In contrast, PB-LP exhibited a lower Py (17.28 kN), although its Pult remained similar (23.48 kN). These findings indicate that while the loop-pin joint improves initial stiffness, its plastic deformation mechanism develops earlier than in PB-L and MB.

2) Moment Capacity

The results show that the moment capacity of the PB-L beam was only marginally higher than that of the MB. Its cracking moment (Mcr = 4.18 kN·m), yield moment (My = 11.98 kN·m), and ultimate moment (Mult = 15.66 kN·m) were very close to the MB values of 4.02 kN·m, 11.94 kN·m, and 15.26 kN·m, respectively. This small difference indicates that the loop connection can effectively replicate the monolithic behavior of the MB. In contrast, the PB-LP beam showed a notably higher cracking moment (Mcr = 6.66 kN·m), approximately 65% greater than the MB, confirming its enhanced initial stiffness consistent with its higher cracking load (Pcr). However, its ultimate moment capacity (Mult = 15.1 kN·m) was slightly lower than both MB and PB-L. This suggests that although the loop-pin joint improves initial stiffness and crack resistance, it does not produce a significant increase in ultimate flexural capacity.

B. Load–Deflection Relationship

The relationship between load (Pcr, Py, Pu) and deflection (Δcr, Δy, Δu) obtained from the flexural tests of the PB-L and PB-LP precast beam joints, as well as the MB as the control specimen, are presented in Figure 5 and Table IV.

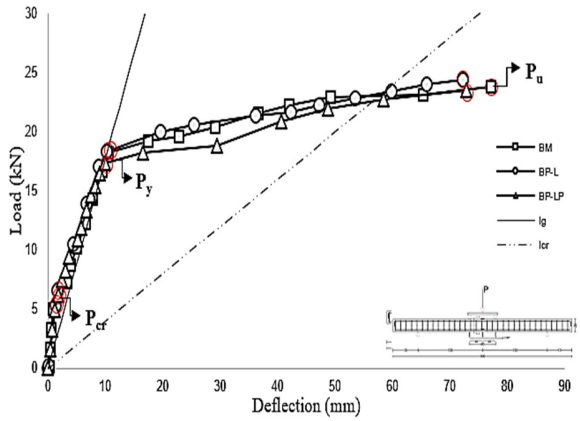

Fig. 5. Load–deflection relationship.

TABLE IV. LOAD AND DEFLECTION

Type	Load (kN)			Deflection (mm)		
	Pcr	Py	Pult	Δcr	Δy	Δult
MB	5.02	18.21	23.74	0.91	10.54	77.11
PB-L	5.29	18.28	24.41	1.25	10.19	72.19
PB-LP	9.42	17.28	23.48	3.66	9.86	72.78

The results show that the MB had the smallest cracking deflection (Δcr = 0.91 mm), whereas the PB-LP exhibited the largest (Δcr = 3.66 mm), indicating that its higher cracking load is associated with a greater deformation demand at crack initiation. The PB-L response (Δcr = 1.25 mm) was intermediate and closely matched that of the MB. At the yield stage, all beams recorded similar deflections of approximately 10 mm, suggesting that the use of precast joints does not significantly influence deformation behavior at yielding. Likewise, the ultimate deflections (Δult) of the three beams were comparable, ranging from 72 mm to 77 mm, showing that overall deformation capacity is maintained regardless of the joint type. The ductility ratios (μ = Δult/Δy) ranged from 7 to 7.4, placing all specimens within the high-ductility category (μ > 4) defined in [20]. These results confirm that both loop and loop-pin connections preserve ductile behavior and provide plastic deformation capacity comparable to that of monolithic beams.

C. Load–Steel Strain Relationship

The load–strain curves of steel, portrayed in Figure 6, illustrate the different behaviors between the MB and the PB-L and PB-LP connections. The measured steel yield strain (εy) values were 2015 με for MB, 1138 με for PB-L, and 530 με for PB-LP. These results indicate that the steel in the loop-pin connection yielded earlier than that in the loop and MBs.

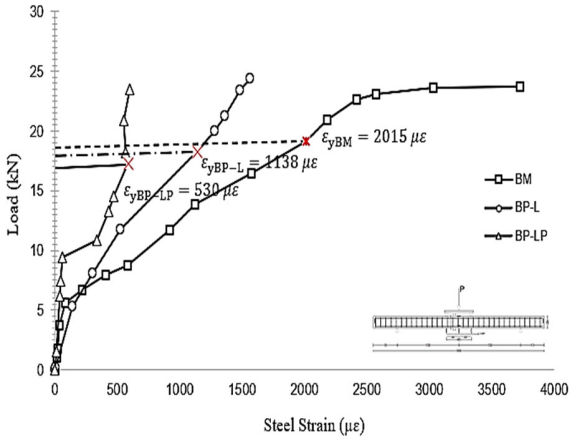

Fig. 6. Load–steel strain relationship.

In the ultimate condition, the differences become more evident. The ultimate loads of the three beams were relatively similar: 23.74 kN for MB, 24.41 kN for PB-L, and 23.48 kN for PB-LP. However, the steel strain at ultimate load showed a significant contrast: 3727 με for MB, 1138 με for PB-L, and only 584 με for PB-LP. This indicates that the MB can accommodate larger steel deformations before failure, whereas the precast beams, particularly PB-LP, tend to reach the ultimate state with lower steel strain.

D. Load–Strain Relationship of Concrete

The load–strain relationship of concrete, displayed in Figure 7, indicates that the concrete yield strain (εy) occurs at different values for each beam type. The PB-L and PB-LP connections reached the yield strain at approximately 981 με, whereas the MB exhibited a higher yield strain of 3080 με. Although the ultimate load capacities of the three beam types were relatively similar (approximately 23 kN–25 kN), the concrete strain behavior showed clear differences. The MB was able to sustain larger concrete deformations before reaching the ultimate condition, while the PB exhibited lower ultimate strains. This indicates that the force transfer mechanism in precast connections, both loop and loop-pin types, causes the concrete to mobilize earlier and approach its ultimate strain limit more quickly compared to the MB.

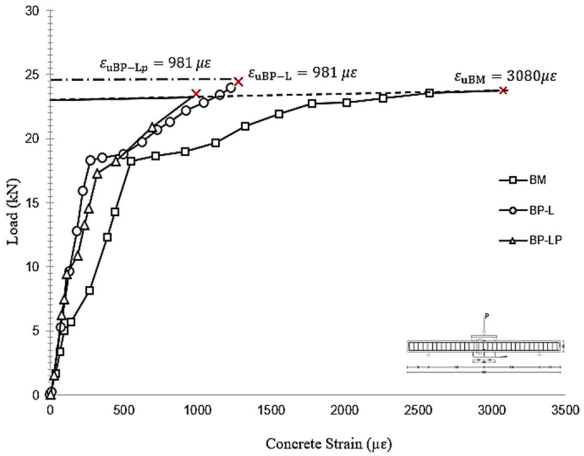

Fig. 7. Load–strain relationship of concrete.

E. Crack Pattern and Failure Mechanism

1) Crack Pattern and Failure Mode of the MB

As shown in Figure 8, the BM exhibited the first crack at a load of 5.02 kN, initiating at the mid-span tensile zone. The crack propagated vertically toward the compression zone as the load increased, forming a typical flexural cracking pattern. With further loading, additional cracks developed along the constant moment region and widened progressively until the beam reached its maximum load. At the ultimate stage, the load-bearing capacity ceased to increase, while deflection continued growing, followed by a sudden drop, indicating flexural failure governed by steel yielding. The observed failure mode confirmed an under-reinforced behavior, where the tensile reinforcement yielded before the concrete crushed.

2) Crack Pattern and Failure Mechanism of the PB-L

As shown in Figure 9, the PB-L specimen exhibited the first flexural crack at a load of 5.29 kN, initiating along the interface between the old concrete and the grouted joint in the mid-span region. With increasing load, additional flexural cracks developed along the constant moment region, following the interface path due to the non-monolithic nature of the connection. This behavior indicates partial bonding between the old concrete and grouting, leading to the formation of wider cracks near the joint. The mechanical behavior of the loop connection was governed by the interaction between the existing concrete, the grout, and the loop reinforcement. The grout formed a mechanical interlock around the loop, improving shear transfer through bond and friction at the interface. However, as loading increased, the specimen experienced bond failure (debonding), evidenced by crack initiation and widening along the interface, while the grout itself remained intact. This behavior is attributed to inadequate surface roughness on the precast concrete interface, which limited frictional confinement.

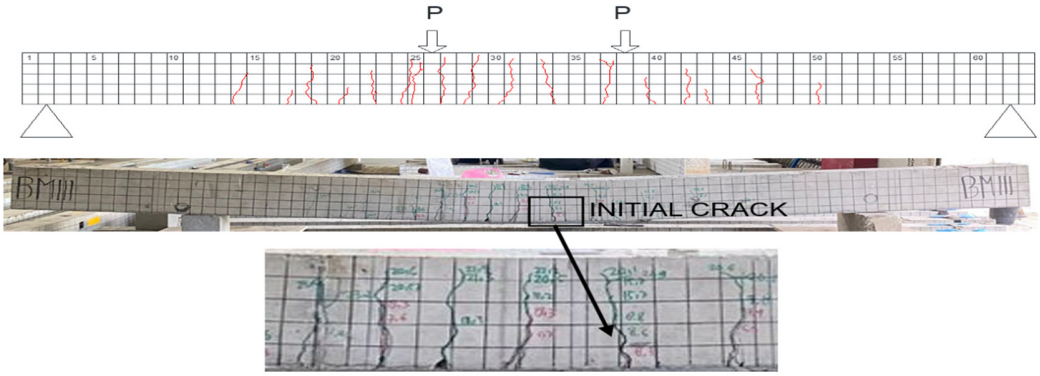

Fig. 8. Crack pattern of MB specimen.

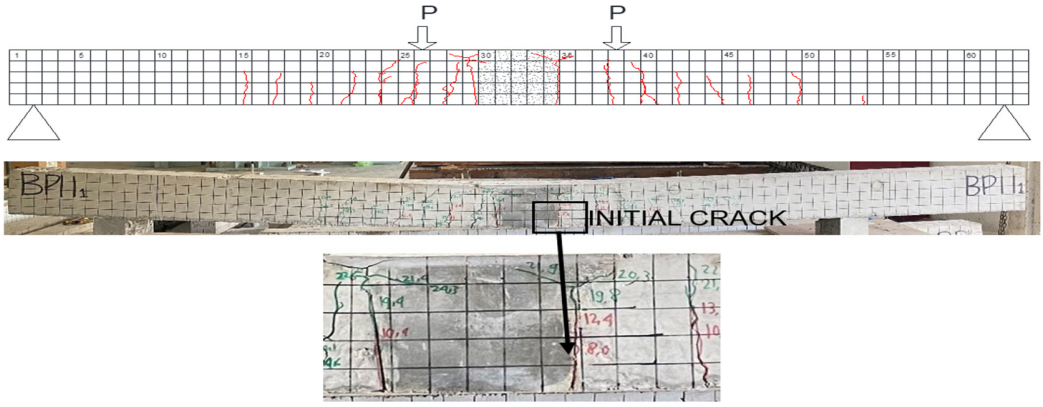

Fig. 9. Crack pattern of the PB-L.

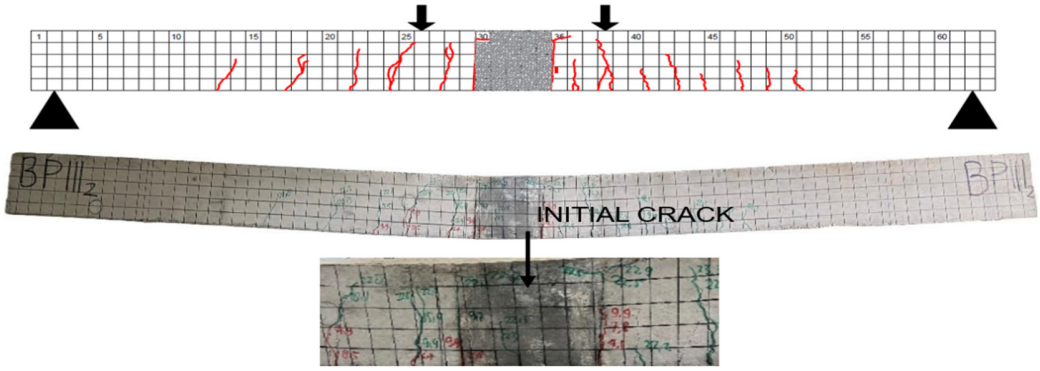

Fig. 10. Crack pattern of the PB-LP.

The failure mode confirmed partial composite action between the old and new concrete, indicating that the joint did not behave fully monolithically. Similar findings were reported in [18], where interface cracking was observed as the primary failure in loop-grouted connections.

3) Crack Pattern and Failure Mechanism of the PB-LP

As illustrated in Figure 10, the PB-LP specimen developed its first crack near the grouted interface at mid-span, initially as a flexural crack and later transitioning into a flexural–shear pattern. The cracks then propagated more uniformly away from the joint region, indicating more effective force transfer compared to the PB-L. The PB-PL configuration created a stronger mechanical interlock, improving bond and friction along the concrete–grout interface. This reduced bond-slip, enhanced shear transfer, and produced a response that more closely resembled monolithic behavior. These observations align with [18, 21, 22], where it was reported that adding mechanical interlocking elements, such as pins or dowel-like bars, to loop connections increases flexural strength, improves shear transfer efficiency, and helps concentrate cracking at the interface. In the PB-LP specimen, the inclusion of the pin further strengthened this interlock, leading to better-controlled interface cracking and a more distributed crack pattern. Overall, PB-LP demonstrated a more controlled and ductile response, confirming the effectiveness of pins in improving force transfer and reducing stress concentrations in loop connections.

F. Discussion

The experimental results show clear differences in flexural behavior between the MB and the two precast connections, PB-L and PB-LP. Among the precast specimens, PB-L most closely replicated the behavior of the MB, particularly in terms of yield and ultimate load capacities. In contrast, PB-LP exhibited higher initial stiffness and a greater cracking load. This increase in stiffness is attributed to the horizontal pin within the loop, which improves mechanical interlock and enhances bond and shear transfer at the concrete–grout interface. By reducing relative slip, this interlock enables the joint to behave more like a monolithic section during the early stages of loading. However, the localized stiffness also leads to higher stress concentration in the grouted region, limiting strain development at larger loads and causing earlier yielding and slightly reduced deformation capacity. The load–deflection response showed that at the cracking stage, PB-LP experienced greater deformation due to its higher cracking load, while MB had the smallest deflection. Despite these differences, the deflections at yield and ultimate conditions were similar across all beam types, averaging 10 mm and 72 mm-77 mm, respectively. The ductility ratios ($\mu = \Delta ult/\Delta y$) ranged between 7 and 7.4, indicating high ductility according to [28]. This confirms that both precast connections can accommodate significant plastic deformation while maintaining stability under flexural loading. The strain results support these findings: MB recorded the highest ultimate steel strain (3727 με), while PB-L and PB-LP were considerably lower (1138 με and 584 με). Similarly, concrete strains in precast specimens reached approximately one-third of those in MB, suggesting earlier stress mobilization that increases stiffness but reduces deformability. These results indicate that the addition of pins improves load transfer and crack control but slightly restrains ductility due to localized stiffness at the joint. Similar behavior was reported in [18, 21, 22], where mechanical interlocking systems enhanced bond strength and force-transfer efficiency while moderating the overall ductile response. The PB-L connection is the most balanced precast option, closely mimicking the behavior of monolithic structures. In contrast, PB-LP provides higher stiffness, better bond efficiency, and greater resistance to cracking, though it slightly reduces deformation capacity. Both types satisfy the ductility requirements for earthquake-resistant structures, making them suitable for low-rise residential buildings in seismic zones. Furthermore, the similarity among the load–deflection curves for all three beams can be explained by their identical reinforcement ratios and comparable moment capacities, which govern the global flexural response. Once yielding occurred, all specimens exhibited similar plastic behavior, indicating that both loop and loop-pin joints effectively transmitted bending and shear forces, resulting in near-monolithic behavior. The overlapping curves, therefore, confirm the high integrity of the grouted joints and the efficiency of the loop and loop-pin systems in maintaining structural continuity.

IV. CONCLUSIONS

Based on the static flexural test results on the MB and PB-L and PB-LP connections, the following conclusions are drawn:

- The PB-LP connection exhibited higher initial stiffness and cracking load capacity than MB and PB-L, though its ultimate moment capacity was slightly lower.
- All beam types achieved ductility ratios of about 7 ($\mu > 4$), indicating high ductility and compliance with seismic design requirements.
- PB-L most closely replicated monolithic behavior, while PB-LP offered greater stiffness and crack resistance.
- Both connection types are suitable for simple, low-cost housing in seismic regions due to their structural reliability and ease of construction.

From a practical perspective, both connection types are suitable for simple building construction in seismic-prone areas, ensuring structural stability while supporting efficient construction processes. The PB-L connection is more suitable for low-cost residential structures that require balanced ductility and ease of assembly, while the PB-LP connection is preferable for applications demanding higher stiffness and enhanced crack control, such as components subjected to higher service load conditions or where deflection limits are critical. The findings of this study provide an important contribution to the development of precast connection systems for earthquake-resistant housing construction. The loop and loop-pin connection systems offer ease of implementation, faster construction time, and structural performance that meets ductility requirements for seismic regions. Future research is proposed to investigate the behavior of these connections under cyclic or seismic loading through experimental testing and numerical simulation, as well as to extend the study to beam–column joints to ensure the reliability of the system in more complex structural configurations.

REFERENCES

[1] "Natural Disasters in Indonesia," *Indonesia Investments*, 2025.

[2] "Welcome - Portal Satu Data Bencana Indonesia." https://data.bnpb.go.id/.

[3] "TINJAUAN PENGGUNAAAN BALOK PRACETAK PADA PEMBANGUNAN GEDUNG," *adoc.pub*. https://adoc.pub/tinjauan-penggunaaan-balok-pracetak-pada-pembangunan-gedung.html.

[4] *PCI Design Handbook, 8th Edition - (MNL-120-17)*. USA: Precast/Prestressed Concrete Institute, 2021.

[5] Rekha and Ravindra, "Prefabricated Concrete Technology- Perspectives And Challenges," *International Journal of Advances in Scientific Research and Engineering (IJASRE), ISSN:2454-8006, DOI: 10.31695/IJASRE*, vol. 3, no. 1 Special issue, pp. 444–452, Aug. 2017, [Online]. Available: https://ijasre.net/index.php/ijasre/article/view/944.

[6] *ACI 550.1R-09 Guide to emulating cast-in-place detailing for seismic design*. USA: American Concrete Institute, 2009.

[7] I. Padang, R. Djamaluddin, H. Parung, and A. Amiruddin, "KAJIAN LITERATUR SISTEM SAMBUNGAN BALOK SLOOF PRACETAK KONSTRUKSI RUMAH SEDERHANA TAHAN GEMPA," *Konferensi Nasional Teknik Sipil (KoNTekS)*, vol. 2, no. 3, 2024, https://doi.org/10.62603/konteks.v2i3.166.

[8] Z. Xu, W. Zhou, and G. Lu, "Experimental study on flexural behavior of precast concrete beams in-span joined with UHPC," *Journal of Building Engineering*, vol. 111, Oct. 2025, Art. no. 113190, https://doi.org/10.1016/j.jobe.2025.113190.

[9] S. Li and W. Chen, "Experimental Study and Theoretical Prediction on the Flexural Behavior of Unbonded, Post-tensioned Precast Beams Made of Recycled Aggregate Concrete," *International Journal of Civil Engineering*, vol. 22, no. 7, pp. 1207–1222, July 2024, https://doi.org/10.1007/s40999-024-00947-4.

[10] X. Nie, D. Huang, L. Zhuang, J. Fan, and N. Deng, "Precast concrete connections for alleviating reinforcement congestion: A state-of-the-art review," *Engineering Structures*, vol. 331, May 2025, Art. no. 119985, https://doi.org/10.1016/j.engstruct.2025.119985.

[11] Y. Yang, C. Xu, J. Yang, and K. Wang, "Experimental study on flexural behavior of precast hybrid UHPC-NSC beams," *Journal of Building Engineering*, vol. 70, July 2023, Art. no. 106354, https://doi.org/10.1016/j.jobe.2023.106354.

[12] H. Zheng, D. Chen, M. Ou, X. Liang, and Y. Luo, "Flexural Behavior of Precast UHPC Segmental Beams with Unbonded Tendons and Epoxy Resin Joints," *Buildings*, vol. 13, no. 7, July 2023, Art. no. 1643, https://doi.org/10.3390/buildings13071643.

[13] A.- Maryoto, "Pengaruh Panjang Sambungan Pada Beton Prategang Segmental Bertulangan Limbah Ban," *Jurnal Teknik Sipil dan Perencanaan*, vol. 19, no. 1, pp. 65–70, July 2017, https://doi.org/10.15294/jtsp.v19i1.9500.

[14] H. A. Tumengkol, R. Irmawaty, H. Parung, and A. Amiruddin, "Precast Concrete Column Beam Connection Using Dowels Due to Cyclic Load," *International Journal of Engineering*, vol. 35, no. 1, pp. 102–111, Jan. 2022, https://doi.org/10.5829/ije.2022.35.01A.09.

[15] S.-D. Dao, "Research on the Estimation of the Flexural Capacity of EPS Lightweight Concrete Panels," *Engineering, Technology & Applied Science Research*, vol. 14, no. 6, pp. 18889–18895, Dec. 2024, https://doi.org/10.48084/etasr.9091.

[16] T. Q. K. Lam and H. E. Ho, "Flexural Behavior of Reinforced Concrete Beams using Recycled Glass as a Sand Substitute," *Engineering, Technology & Applied Science Research*, vol. 15, no. 2, pp. 22159–22165, Apr. 2025, https://doi.org/10.48084/etasr.10429.

[17] H. Riyanto, "Perilaku Statis Struktur Beton Pracetak Dengan Sistem Sambungan Basah," *Jurnal Teknik Sipil*, vol. 1, no. 1, Oct. 2010, https://doi.org/10.36448/jts.v1i1.251.

[18] Q.-T. Nguyen, T. Maki, H. Mutsuyoshi, and Y. Ishihara, "Flexural Behavior of Precast Concrete Slab Connections using Loop Steel Bars and Mortar," *Journal of Advanced Concrete Technology*, vol. 21, no. 6, pp. 436–449, 2023, https://doi.org/10.3151/jact.21.436.

[19] K. Hu, C. Zhu, X. Shi, and Y. Zhong, "Experiment on Flexural Fatigue Performance of Precast Bridge Deck Joints with Loop Connections," *Applied Sciences*, vol. 14, no. 2, Jan. 2024, Art. no. 566, https://doi.org/10.3390/app14020566.

[20] K. Wang, G. Liu, C. Wang, and F. Wang, "Tensile analysis of loop joints with different overlap lengths," *Journal of Asian Architecture and Building Engineering*, vol. 24, no. 4, pp. 2616–2628, July 2025, https://doi.org/10.1080/13467581.2024.2357760.

[21] Y. Wu, S. Hu, M. Li, and B. Rong, "Flexural Behavior of Wet Joints with Contact U-Bars," *Buildings*, vol. 15, no. 6, Jan. 2025, Art. no. 855, https://doi.org/10.3390/buildings15060855.

[22] K. C. G. Ong, J. B. Hao, and P. Paramasivam, "Flexural Behavior of Precast Joints with Horizontal Loop Connections," *Structural Journal*, vol. 103, no. 5, pp. 664–671, Jan. 2006, https://doi.org/10.14359/16918.

[23] *SNI 2847-2019 Persyaratan Beton Struktural Untuk Bangunan Gedung SNI 1726-2019 Persyaratan Beton Struktural Untuk Bangunan Gedung*. Indonesia: Badan Standardisasi Nasional, 2019.

[24] *SNI 1974:2011 Cara uji kuat tekan beton dengan benda uji silinder*. Indonesia: Standar Nasional Indonesia, 2011.

[25] *SNI 2052-2017 Baja tulangan beton*. Indonesia: Standar Nasional Indonesia, 2017.

[26] *SNI 03-6825-2002 Metode pengujian kekuatan tekan mortar semen portland untuk pekerjaan sipil*. Indonesia: Standar Nasional Indonesia, 2002.

[27] *SNI 4431-2011 Cara Uji Kuat Lentur Beton Normal Dengan Dua Titik Pembebanan*. Indonesia: Standar Nasional Indonesia, 2011.

[28] *ASCE/SEI 41-17 Seismic Evaluation and Retrofit of Existing Buildings*. USA: American Society of Civil Engineers, 2017.